International Journal of Heat and Mass Transfer 52 (2009) 1540–1543

Contents lists available at ScienceDirect

International Journal of Heat and Mass Transfer

journal homepage: www.elsevier.com/locate/ijhmt

Pulsed photothermal heating of the media during bubble generation around gold nanoparticles

Dmitri Lapotko

A.V. Lykov Heat and Mass Transfer Institute, 15 P. Brovka Street, Minsk 220072, Belarus

ARTICLE INFO

Article history:
Received 18 July 2008
Available online 1 October 2008

Keywords:
Photothermal
Bubble
Gold nanoparticles
Thermal lens

ABSTRACT

Pulsed laser induced heating of the transparent media with light-absorbing nanoparticles (NP) in water and in living cells was experimentally studied with photothermal microscopy and thermal lens methods. At low laser-induced temperatures of the NPs and without vapor bubble generation the media was heated by NPs due to thermal diffusion. At higher laser-induced temperatures of the NPs that have caused the generation of vapor bubbles around NPs no heating of the media outside the bubbles and after their collapse was observed. This effect of "cold" generation of the bubbles is associated with NP properties and was not observed during bubble generation in homogeneously heated light-absorbing media under equal conditions.

1. Introduction

Plasmon resonance properties of metal nanoparticles (NP) provide efficient conversion of optical energy into thermal one at nanoscale. Thermal output of NP depends upon (1) their optical absorbance cross-section, (2) laser fluence and pulse duration, and (3) heat transfer between the NP and surrounding (bulk) media. Primary photothermal (PT) effect of laser-NP interaction is the thermalization of NP [1,2]. Secondary PT effects include the bulk heating of surrounding media due to thermal diffusion [1–6] and the vapor bubble generation if the temperature of the media exceeds evaporation threshold [3,7–9]. While the primary PT effects were extensively studied, the secondary PT effects are less explored. On the other hand in any thermal applications of NPs (especially biomedical ones when NPs heat the living cells and tissues) it is important to understand and to control the spatial and temporal behavior of laser-induced temperature in the bulk media around NP. With the focus on the pulsed laser-NP interaction we have experimentally studied bulk secondary PT effects for the microvolumes of water suspensions of gold NPs, in homogeneous optically absorbing solutions, and in individual living cells where optical absorbance was provided by localized gold nanoparticles (cancer cells) and by quite homogeneously distributed light-absorbing hemoglobin (red blood cells).

2. Methods and materials

As the sample we have employed the water suspension of gold NP, which volume was confined by laser beam aperture (12 μm) and by the height of the cuvette (120 μm) (Fig. 1). Three types of gold NPs were studied: 30 nm spheres (#15706, Ted Pella, Inc., Redding, CA), gold nanoshells (NS) of 170 nm were prepared as described in [10] and 14 × 45 nm gold nanorods (NR) were prepared as described in [11]. An average inter-particle distance at the concentration being used was 1.7 μm. Water suspension of NPs was irradiated with a single 10 ns, 532 nm laser pulse, which fluence varied from 0.05 to 15 J/cm^2 so to provide for each type of the studied NPs the heating of the water (bulk media) below and above vaporization thresholds.

Two types of living cells were studied: intact red blood cells and lung cancer A549 culture cells with internalized gold NP (170 nm nanoshells). In red blood cells the main optical absorber and the heat source is the hemoglobin that is homogenously distributed within the cell volume at micrometer scale. This type of cells was used to study bulk heating PT effect for the case when the whole media is heated and thus produces the bubbles. In A549 cells the optical absorption was provided only by the NPs that were localized in the cells and thus have acted as point heat sources.

Our experimental set up has employed the developed by us time-resolved laser microscope [12,13] and 10 ns, 532 nm pulsed laser (LS-2132, Lotis TII, Minsk, Belarus) for optical excitation of the samples. The fluence of laser pulse was obtained through (1) measuring pulse energy with custom photodiode that was calibrated with Ophir energy meter (PE10-SH, Ophir Optronics, Ltd., Israel) and (2) measuring the diameter of laser spot in the sample plane with CCD image detector (DL-658M-TIL, Andor Technology, Ireland) at the pixel amplitude level being 0.5 of the maximum. The concentrations of NP suspensions were 2.5 * 10^{11}/ml for all samples and this corresponds to an average distance between NP centers being 1.7 μm. This distance is much larger than thermal

E-mail address: Ld@hmti.ac.by.

0017-9310/$ - see front matter © 2008 Elsevier Ltd. All rights reserved.
doi:10.1016/j.ijheatmasstransfer.2008.08.010

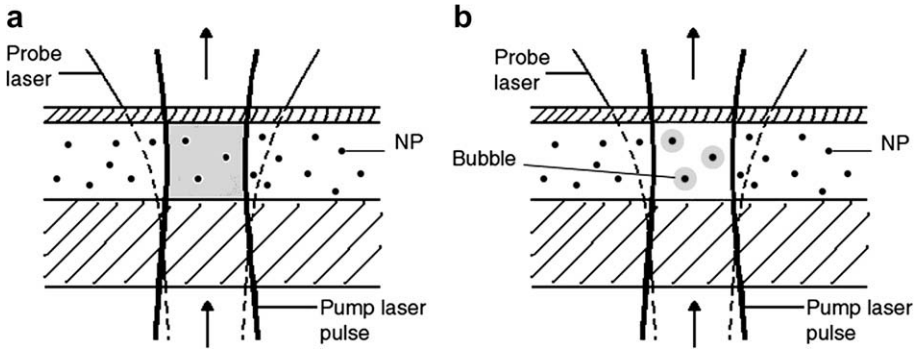

Fig. 1. Experimental model: (a) laser-induced heating of the volume with light-absorbing nanoparticles without bubble generation, (b) generation of laser-induced bubbles around gold nanoparticles; single pump laser pulse: 532 nm, 10 ns.

diffusion radius (l_d) for 10 ns pulse, which was estimated to be 0.2 μm as defined in [14]:

$$l_d = \sqrt{24^* \; t^*_{pump} \; \chi} \tag{1}$$

where t_{pump} is the laser pulse length (10 ns) and χ is the thermal diffusivity of the water (1.37×10^{-7} m^2 c^{-1}).

This condition ensured that the PT phenomena develop around single NPs and without any group effects. On the other hand the volume that was exposed to laser pulse contained approximately 2700 particles that provided bulk secondary heating due to thermal diffusion from NPs to the water or to the cellular microenvironment. It should be noted that the characteristic thermal diffusion time for all NPs being used is much shorter (less than 1 ns) than the duration of laser pulse. This provided bulk heating of the microvolume.

PT heating and bubbles were optically detected in the sample with the two methods. The time course of the volume-averaged laser-induced temperature was registered with the thermal lens method [12,15] with continuous probe laser beam (633 nm, diameter 16 μm in the sample plane). The probe beam was directed through an axial aperture into photodetector (PDA10A, Thorlabs Inc., Newton, NJ) after passing through NP suspension. Output electrical signal of the photodetector was digitized with 4 ns temporal resolution (DSO-250 USB, Qingdao Hatek Electronic, Ltd., China) and was analyzed as PT response of the suspension to the pump laser pulse. The second optical method employed time-resolved phase-contrast imaging of the heated volume with additional 10 ns laser pulse at 750 nm that was generated with Ti-Sa laser (LT-2211, Lotis TII, Minsk, Belarus) and was delayed for 20 ns relatively to excitation pulse for the illumination of the sample. Imaging was realized with the above mentioned CCD camera and 40× microscope objective. Obtained image showed the location of heated areas at the time delay of 20 ns after exposure to laser pulse. Though we did not calibrate our methods for absolute measurements they nevertheless allowed to detect and to distinguish the areas with the temperature being different from the ambient temperature outside laser aperture and the vapor bubbles due to their specific gas–liquid boarder.

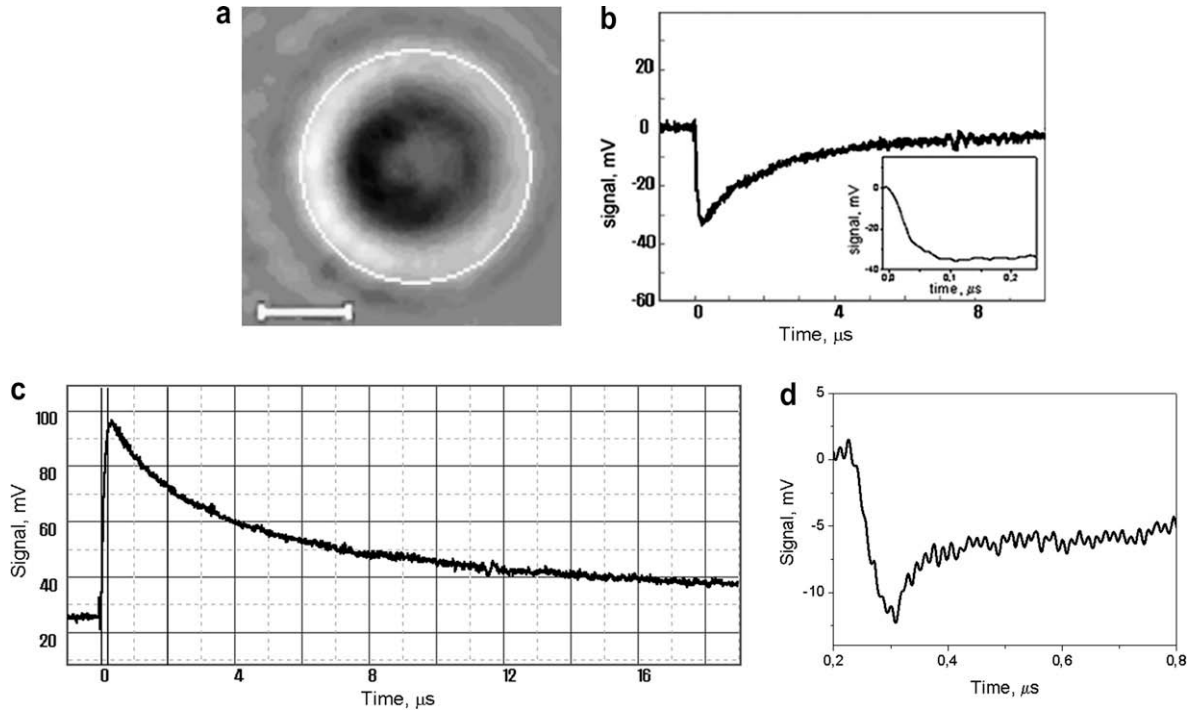

Fig. 2. Time-resolved image (a) and time-responses (b–d) during exposure to a single pump laser pulse (532 nm, 10 ns) of the volume of water suspension with light-absorbing gold nanorods (a and b), individual red blood cell (c) and individual cancer cell A549 with gold nanoshells (d) at laser fluence levels below bubble generation threshold. Image scale bar is 4μm, *Y* axis is for the output of photodetector (mV). The insert in (b) shows the front of the response with high temporal resolution.

3. Results and discussion

3.1. Photothermal effect without bubble generation

At relatively low laser pulse fluencies the main observed PT effect was the heating of the whole space occupied by NP water suspension (Fig. 1a) within the aperture of pump laser beam (shown as the dark image area at Fig. 2a). PT response was obtained simultaneously for the same area of the sample (Fig. 2b) and it yielded: (1) rapid increase of the temperature of the whole irradiated volume followed by exposure to pump laser pulse and (2) gradual cooling of this volume during 3 μs due to heat transfer to outer media outside irradiated volume. All studied NPs have caused similar bulk heating effect at the matching levels of laser pulse fluencies. The laser-induced bulk temperature reaches for its maximum in 30–40 ns (Fig. 2b). This time is required for heating the interparticle space (water) due to thermal diffusion from initially heated NPs. The shape of the decay curve is in agreement with the theory of thermal diffusion [15,16]. Using experimentally obtained cooling time we have estimated with (1) the characteristic diameter of the heated volume to be 8 μm. This estimate is quite close to the size of the dark (i.e. heated) area as shown at Fig. 2(a) and also is slightly smaller than the diameter of the excitation laser beam (12 μm).

Individual living cells with homogeneously distributed absorber (hemoglobin in red blood cells) and lung cancer cells A549 with locally internalized light-absorbing gold nanoparticles have yielded similar heating-cooling responses to irradiation with single laser pulse (Fig. 2c and d). The both responses indicated the increase of cell temperature due to laser-induced heating of the hemoglobin in red blood cell and of gold NPs in A549 cells. The cooling patterns indicated the structural difference of the heat sources in those cells. Red blood cells have yielded gradual cooling within 8–10 μs (Fig. 2c), which corresponds to the cooling of the whole cellular volume. The response obtained from A549 cell has indicated two-step process (Fig. 2d): initial fast cooling that is associated with the heat transfer from the heated NPs to intracellular space and secondary slow cooling of relatively large cancerous cell due to heat transfer to surrounding media. The latter process was measured to take 10-20 μs and is not fully shown at Fig. 2d. An increase of laser fluence has caused nearly linear increase of the maximal amplitudes of the PT responses for all studied NPs and cells. This is in line with (1) the mechanism of heat generation by light-absorbing NP [1,2] and with (2) classical theory of thermal diffusion [16]. Such trend was observed up to the fluencies that induced vapor bubbles.

3.2. Heating of the bulk media during bubble generation

The vapor bubbles were detected in water suspensions of NPs at the thresholds of laser pulse fluence being: 11.0 J/cm^2 for gold rods (Fig. 3), 90 mJ/cm^2 for gold shells, 3.0 J/cm^2 for gold spheres, 4.1 J/cm^2 for red blood cells, and 0.68 J/cm^2 for A549 cells. The bubbles created local positive (white) spots with the diameter about 1 μm in the time-resolved images (Fig. 3a) and specific and strong symmetrical PT responses of NPs (Fig. 3b) due to optical scattering of the probe beam by the bubbles. PT responses show the bubble lifespan that includes the expansion to the maximal diameter and the follow up collapse with the total lifetime being 50 ns for the gold rods (Fig. 3b), 20 ns for gold spheres, 200 ns for the gold shells, 350 ns for red blood cells (Fig. 3d), and 300 ns for A549 cells (Fig. 3e). Corresponding time-resolved images of the bubbles generated around gold nanorods showed that the bubbles did not spatially overlap and were localized within the aperture of the pump laser beam (Fig. 3a).

The most important obtained result was that the amplitude of registered PT responses returned back to the initial (base) level immediately after the collapse of the bubble (Fig. 3b and e) both in NP suspensions and in A549 cells. Also the non-bubble areas of the suspension inside laser aperture (Fig. 3a) did not show

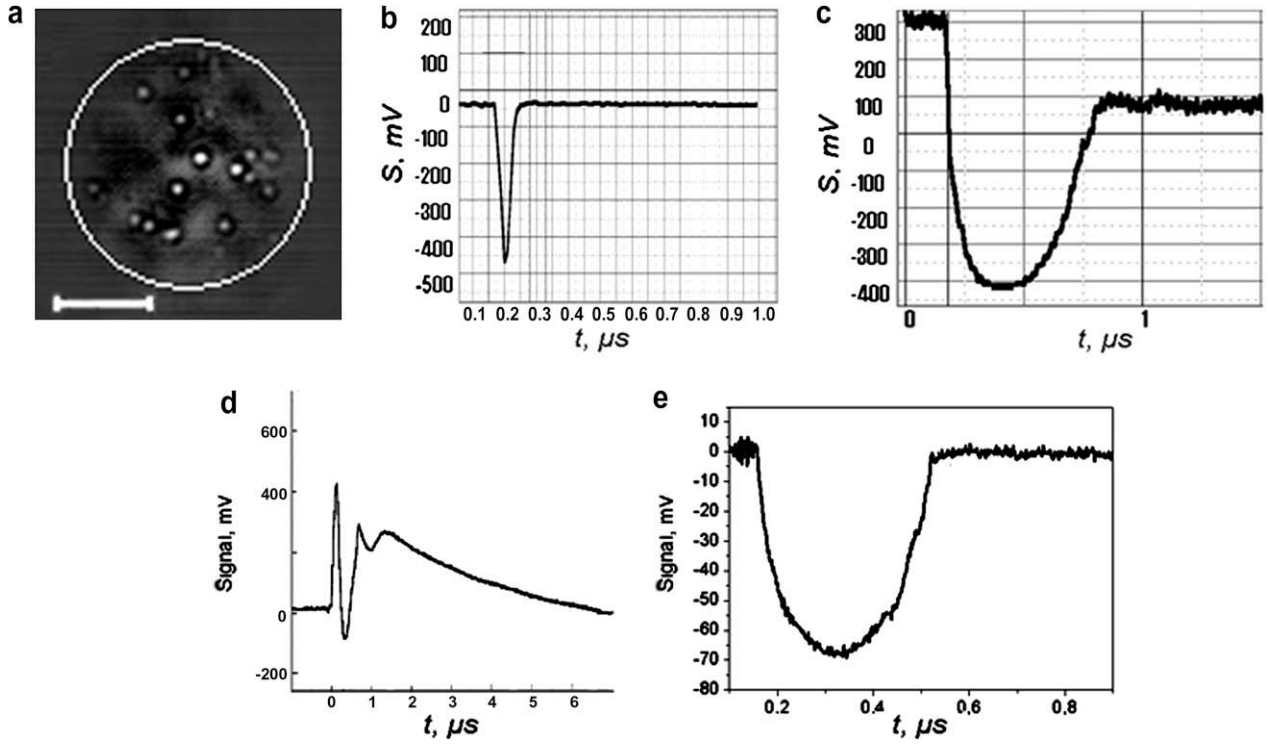

Fig. 3. Time-resolved image (a) and time-responses (b–e) of laser-induced vapor bubbles during exposure to a single pump laser pulse (532 nm, 10 ns) at the fluencies above bubble generation thresholds: a and b – gold nanorods 14 × 45 nm in water, c – light-absorbing homogenous solution of neutral red dye, d – individual red blood cell, e – individual cancer cell A549 with gold nanoshells. Image scale bar is 4 μm, *Y* axis is for the output of the photodetector (mV).

significant deviation from the background level. Similar results were observed for all types of studied NPs. These mean that here was no detectible laser-induced heating of the bulk media outside the bubbles during their development and immediately after the bubble collapse like it was observed for the same objects at lower laser fluencies. Despite of increased deposition of the energy the thermal effects were confined temporally and spatially by the bubbles. This result was quite unexpected as it may not match directly the First Law of Thermodynamics: the more energy is deposited (absorbed by gold NPs), the more heat is released. Generation of the bubbles certainly means that the bulk media surrounding the NPs is locally heated above the bubble generation threshold. But for the larger scale it seems like the bubbles create "thermal insulation" effect for the surrounding media and concentrate all thermal energy inside. Also we did not observe any significant oscillation of the bubble after its collapse, which implies that bubble dynamics is not truly adiabatic. After the bubble collapse a certain amount of thermal energy is locally dissipated and it should produce detectible PT response but we have never observed such secondary heating effect.

To understand the discovered "no bulk heating" effect we have made several additional experiments. First, we have irradiated NP suspension with the train of the two equal pump laser pulses delayed for 20 ns so to check optical scattering effect of the bubble. In case of strong optical scattering by the bubble the effect of second pulse must be weaker than that of the first pulse. Applied delay allowed the time for the bubble to develop after the first laser pulse. PT response obtained from the suspension of gold nanorods (not shown) has yielded the increase of the lifetime of the resulting bubble relatively to that of the bubble generated only with the one pulse (Fig. 3b). Therefore optical shielding effect of the bubble cannot be used as the main explanation of "no bulk heating" effect.

Next we have generated the bubbles in light-absorbing homogenous solutions of neutral red dye and in red blood cells. The both objects had no localized heat sources such as NPs and have produced the bubbles due to the heating of their bulk media. Obtained PT responses clearly showed the bulk heating of the media during and after the generation of the bubbles (Fig. 3d and e). The amplitudes of the PT response after the collapse of the bubbles in those samples did not return to the baseline level clearly indicating increased residual bulk temperature. In these two samples the heat is supposed to be relatively uniformly generated in the whole irradiated volume and there were no local heat sources.

Therefore the reported above "no bulk heating" effect is specific to the generation of vapor bubbles around locally heated NPs. The effect was similar for individual living cells and water suspensions of the NPs of three different types. Initial laser-induced temperature of gold NPs is supposed to be very high (even exceeding gold melting threshold) so to provide the formation of the bubble nuclei around NP. Further heat transfer between super-heated NP and the bulk media does not match heat diffusion model (though this model perfectly explains low-temperature results) and is apparently influenced by the process of nano-bubble generation. Furthermore obtained results bring several questions: (1) where does the energy of the bubble go after its collapse providing that the bubble dynamics is not fully adiabatic? (2) Can we employ the mechanisms of the viscous damping of the bubble at a nanoscale and/or of the generation of acoustic waves to explain further conversion of the energy of the bubble? Discussion of those issues is beyond the scope of this communication, which was focused on the reporting new experimental results. The explanation of the discovered effect is the subject of ongoing work and should involve totally new model of heat-transfer at nanoscale.

4. Conclusions

Based on the obtained experimental results we may conclude that the photothermal properties of transparent suspensions of light-absorbing gold nanoparticles are similar to those of homogeneous light-absorbing fluids at low level of laser fluence when laser-induced heating does not cause the bubbles. The heat deposited in NPs is eventually transferred into surrounding media such as water or intracellular environment. But at higher laser fluencies and during the generation of photothermal vapor bubbles around light-absorbing nanoparticles no detectible heating of the bulk transparent media occurs outside the bubbles. Obtained results were similar for water suspensions of three different types of gold nanoparticles such as the spheres, rods and shells, and also for the living cells. We may therefore conclude about unique and interesting photothermal properties of gold nanoparticles when they act as a pulsed heat sources at nanoscale in the two-phase (liquid–vapor) conditions.

Acknowledgements

The author thanks Professors Jason Hafner and Rebekah Drezek (Rice University, Houston, TX) for their help with gold nanorods and nanoshells that they provided for the experiments.

References

[1] G. Hartland, Phys. Chem. Chem. Phys. 6 (2004) 5263.
[2] S. Link, M. El-Sayed, Int. Rev. Phys. Chem. 19 (2000) 409.
[3] H. Petrova, M. Hu, G. Hartland, J. Phys. Chem. 221 (2007) 361.
[4] R. Anderson, J. Parrish, Science 220 (1983) 524.
[5] C. Pitsillides, E. Joe, X. Wei, R. Anderson, C. Lin, Biophys. J. 84 (2003) 4023.
[6] A. Govorov, H. Richardson, NanoToday 2 (2007) 30.
[7] L. Francois, M. Mostafavi, J. Belloni, J. Delaire, Phys. Chem. Chem. Phys. 3 (2001) 4965.
[8] A. Plech, F. Springer, C. Dahmen, G. von Plessen, V. Kotaidis, J. Chem. Phys. 124 (2006) 184702.
[9] B. Gersman, Proc. SPIE 3902 (2000) 41.
[10] C. Loo, A. Lowery, N. Halas, J. West, R. Drezek, Nano Lett. 5 (2005) 709.
[11] H. Liao, J. Hafner, Chem. Mater. 17 (2005) 4536.
[12] D. Lapotko, G. Kuchinsky, in: F. Scudiery, M. Bertolotti (Eds.), Photoacoustica and Optothermal Phenomena, AIP, Rome, 1998, pp. 184–186.
[13] D. Lapotko, Lasers Surg. Med. 38 (2006) 240.
[14] L. McKenzie, Phys. Med. Biol. 35 (1990) 1175.
[15] D. Lapotko, E. Lukianova, A. Shnip, J. Biomed. Opt. 10 (2005) 014006.
[16] H. Carslaw, J. Jaeger, Conduction of Heat in Solids, 2nd ed., Clarendon Press, Oxford, 1959.